

Large N Expansion for Strongly-coupled Boson-Fermion Mixtures

Kenji Maeda*

Department of Physics, University of Tokyo, Tokyo 113-0033, Japan

revised in August 14, 2021

Abstract

We study a many-body mixture of an equal number of bosons and two-component fermions with a strong contact attraction. In this system bosons and fermions can be paired into composite fermions. We construct a large N extension where both bosons and fermions have the extra large N degrees of freedom and the boson-fermion interaction is extended to a four-point contact interaction which is invariant under the $O(N)$ group transformation, so that the composite fermions become singlet in terms of the $O(N)$ group. It is shown that such $O(N)$ singlet fields have controllable quantum fluctuations suppressed by $1/N$ factors and yield a systematic $1/N$ -expansion in terms of composite fermions. We derive an effective action described by composite fermions up to the next-to-leading-order terms in the large N expansion, and show that there can be the BCS superfluidity of composite fermions at sufficiently low temperatures.

*Email: kmaeda@nt.phys.s.u-tokyo.ac.jp

1 Introduction

The study of boson-fermion mixtures has a long history originating from the analysis of dilute solutions of ^3He atoms in superfluid ^4He [1]. For a weakly-coupled boson-fermion mixture, it is known that the density fluctuation of the bosonic background induces an attraction between the fermions, which enhances the transition temperature to the BCS superfluidity or leads to fermionic superfluidity even without a bare attractive potential between fermions [2, 3]. On the other hand, in the strong coupling regime, it is possible to form bound states between bosons and fermions, called composite fermions (CFs) or simply dimers (tightly-bound molecules) [4]. Therefore, phase structures in the strong coupling regime may differ from those in the weak coupling regime, and it is expected that there occurs the superfluidity of CFs at low temperatures [5], which greatly motivates us to model superfluid hadronic matters in dense QCD in terms of boson-fermion mixtures where small size diquarks correspond to the bosons, unpaired quarks to the fermions, and the extended nucleons are regarded as the CFs [6–8].

Recent developments in atomic experiments have made it possible to realize boson-fermion mixed gases in the laboratory. Atomic interaction between different species can be tuned with the use of Feshbach resonance techniques [9–11]. Recently, the formation of heteronuclear Feshbach molecules has been observed in a boson-fermion mixture of ^{87}Rb and ^{40}K atomic vapors in a 3D optical lattice [12] and in an optical dipole trap [13].

From a theoretical point of view, there are several non-perturbative studies on nonrelativistic atomic gases. In particular, the large N method provides a systematic expansion with the corresponding diagrammatic representations, and the applicability of its results to the physical cases at $N = 1$ can in principle be tested by systematic estimates of higher-order contributions. The transition temperature of the dilute interacting Bose gas has been calculated with the use of $1/N$ -expansion [14, 15]. Also, the $1/N$ -expansion for the nonrelativistic Fermi gases has been developed in Refs. [16–18]. A review of large N expansions in $O(N)$ and $U(N)$ quantum field theories, which deals with non-perturbative aspects of critical phenomena, may be found in Ref. [19]. However, detailed studies of the strongly-coupled boson-fermion mixtures in the large N method are still missing.

In this paper we present an extensive study of a large N extension for a model of strongly-coupled boson-fermion mixtures originally proposed in Ref. [7]. We establish the $1/N$ -expansion in a theory of CFs which is equivalent to the original boson-fermion mixed system. We also derive an effective action of CFs up to the next-to-leading-order terms in the large N expansion, and show that there can be the BCS superfluidity of CFs at low temperatures.

Our paper is organized as follows. In Sect. 2, we construct a large N extension of strongly-coupled boson-fermion mixtures at finite temperature and density based on the imaginary-time formalism. In Sect. 3, we rewrite the boson-fermion partition function in terms of CFs with the use of an auxiliary-field method. We derive an action functional of CFs and find a systematic expansion, $1/N$ -expansion, which is equivalent to a loop expansion with respect to the CF fields. In Sect. 4, the $1/N$ -expansion is employed to calculate the leading-order (LO) and the next-to-leading-order (NLO) terms in our CF action. We also derive a low-energy effective theory of CFs, and find that it reduces to a two-component free Fermi gas in the LO analysis, and to a weakly-interacting two-component Fermi gas up to the NLO study, which yields the superfluidity of CFs at sufficiently low temperatures. Finally, in Sect. 5 we discuss the application of boson-fermion mixtures to dense QCD. In Appendix A, we give explicit forms of Fourier transformations especially for the proper vertex functions of CF fields. Appendix B provides details on the derivative expansion of the inverse propagator of CFs.

2 Formulation of large N boson-fermion mixtures

In our model, we treat bosons and two-component fermions using a nonrelativistic gas model of the boson-fermion mixture where bosons and fermions interact through a four-point contact interaction. We start from a Hamiltonian density of our boson-fermion mixture in three spatial dimensions,

$$\begin{aligned} \mathcal{H} = & \sum_{i=1}^N \phi_i^\dagger(x) \left(-\frac{\nabla^2}{2m_b} - \mu_b \right) \phi_i(x) + \sum_{i=1}^N \sum_{\sigma=\uparrow,\downarrow} \psi_{\sigma i}^\dagger(x) \left(-\frac{\nabla^2}{2m_f} - \mu_f \right) \psi_{\sigma i}(x) \\ & + \frac{g_{bf}}{N} \sum_{i,j=1}^N \sum_{\sigma=\uparrow,\downarrow} \phi_i^\dagger(x) \psi_{\sigma i}^\dagger(x) \phi_j(x) \psi_{\sigma j}(x), \end{aligned} \quad (1)$$

where ϕ_i is the bosonic and $\psi_{\sigma i}$ is the fermionic field. We label the two internal states of the fermions by pseudospin indices $\sigma = \uparrow, \downarrow$ and extra large N indices of bosons and fermions by $i, j = 1, 2, \dots, N$. We assume that two different pseudospin states have the same mass and chemical potential (number density) and that the boson-fermion interaction is independent of pseudospin states. Setting $N = 1$ yields the same Hamiltonian density as in our previous work [7], though here we neglect interactions between same species by assuming that the boson-fermion interaction is much stronger than the others. To make our analysis simple, we focus on an equally populated mixture of bosons and fermions, which means for each i we have n bosons and n fermions with an equal population in their number densities: $n_{bi} = n_{\uparrow i} + n_{\downarrow i} = n$ and $n_{\uparrow i} = n_{\downarrow i} = n/2$. Also, we introduce total boson (fermion) number density as $n_{\text{tot}} = Nn$.

The bare boson-fermion coupling g_{bf} is related to the s-wave scattering length in the vacuum a_{bf}

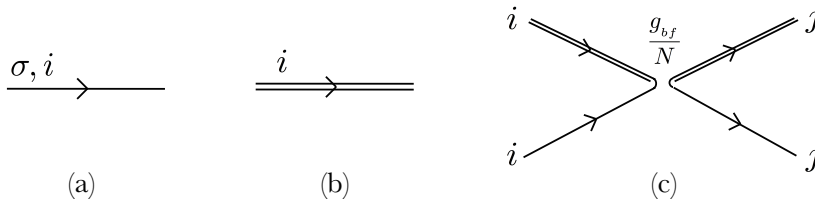


Figure 1: Feynman diagrams for the boson-fermion mixture described by the action Eq.(4). The indices for large N degrees of freedom are explicitly shown by i or j . (a) The single line denotes one of propagators for two-component fermions labeled by σ and i , (b) the double line corresponds to the propagator for bosons, and (c) the interaction vertex between bosons and fermions is represented by the empty space associated with a suppression factor g_{bf}/N in terms of the $1/N$ -expansion.

by the following relation [20],

$$\frac{m_R}{2\pi a_{bf}} = \frac{1}{g_{bf}} + \int_{|\mathbf{k}| \leq \Lambda} \frac{d\mathbf{k}}{(2\pi)^3} \frac{1}{\varepsilon_b(\mathbf{k}) + \varepsilon_f(\mathbf{k})}, \quad (2)$$

where $\varepsilon_b(\mathbf{k}) = \mathbf{k}^2/2m_b$ and $\varepsilon_f(\mathbf{k}) = \mathbf{k}^2/2m_f$ are the kinetic energies of the single boson and fermion, respectively, $m_R = m_b m_f / (m_b + m_f)$ is the boson-fermion reduced mass, and Λ is a high-momentum cutoff of our model which sets a minimum atomic scale $r_0 = (2\Lambda/\pi)^{-1}$. For a simple notation, we will omit the constrain to the momentum-integral; $|\mathbf{k}| \leq \Lambda$.

The partition function at finite temperature becomes

$$Z = \int \left(\prod_{i=1}^N \mathcal{D}\phi_i^* \mathcal{D}\phi_i \right) \left(\prod_{i=1}^N \prod_{\sigma=\uparrow,\downarrow} \mathcal{D}\bar{\psi}_{\sigma i} \mathcal{D}\psi_{\sigma i} \right) \exp \left\{ -S[\phi_i^*, \phi_i, \bar{\psi}_{\sigma i}, \psi_{\sigma i}] \right\}, \quad (3)$$

expressed by an imaginary-time functional integral over bosonic fields ϕ_i, ϕ_i^* and fermionic Grassmann fields $\psi_{\sigma i}, \bar{\psi}_{\sigma i}$ with the corresponding action functional of our boson-fermion mixture:

$$\begin{aligned} S[\phi_i^*, \phi_i, \bar{\psi}_{\sigma i}, \psi_{\sigma i}] &= \int dx \sum_{i=1}^N \phi_i^*(x) \left(\frac{\partial}{\partial \tau} - \frac{\nabla^2}{2m_b} - \mu_b \right) \phi_i(x) \\ &+ \int dx \sum_{i=1}^N \sum_{\sigma=\uparrow,\downarrow} \bar{\psi}_{\sigma i}(x) \left(\frac{\partial}{\partial \tau} - \frac{\nabla^2}{2m_f} - \mu_f \right) \psi_{\sigma i}(x) \\ &+ \int dx \frac{g_{bf}}{N} \sum_{i,j=1}^N \sum_{\sigma=\uparrow,\downarrow} \phi_i^*(x) \bar{\psi}_{\sigma i}(x) \phi_j(x) \psi_{\sigma j}(x). \end{aligned} \quad (4)$$

Here for simple descriptions we have used notations: $x = (\mathbf{x}, \tau)$, $\int dx = \int_0^\beta d\tau \int d\mathbf{x}$, and $\hbar = k_B = 1$. Figure 1 shows the corresponding Feynman diagrams for the boson-fermion mixture, especially focused on the large N degrees of freedom.

3 From boson-fermion mixtures to composite fermions

In strongly-coupled boson-fermion mixtures characterized by the positive and small scattering length ($0 < n_{\text{tot}}^{1/3} a_{bf} \ll 1$), we expect that bosons and fermions form bound dimers or *composite fermions*

(CFs) [4, 5] and that low-energy phenomena can be described by an effective theory of these CFs. For this purpose, we introduce fermionic auxiliary fields $F'_\sigma(x)$ and $\bar{F}'_\sigma(x)$ by inserting the following identity into the partition function:

$$1 = c \int \left(\prod_{\sigma=\uparrow,\downarrow} \mathcal{D}\bar{F}'_\sigma \mathcal{D}F'_\sigma \right) \exp \left\{ \frac{N}{g_{bf}} \int dx \sum_{\sigma=\uparrow,\downarrow} \bar{F}'_\sigma(x) F'_\sigma(x) \right\}, \quad (5)$$

where c is a normalization constant [21]. We also define shifted fields $F_\sigma(x)$ and $\bar{F}_\sigma(x)$ as

$$F'_\sigma(x) = \frac{g_{bf}}{N} \sum_{i=1}^N \phi_i(x) \psi_{\sigma i}(x) + F_\sigma(x), \quad (6)$$

$$\bar{F}'_\sigma(x) = \frac{g_{bf}}{N} \sum_{i=1}^N \phi_i^*(x) \bar{\psi}_{\sigma i}(x) + \bar{F}_\sigma(x). \quad (7)$$

Note that the shifted fields $F_\sigma(x)$ and $\bar{F}_\sigma(x)$ can be considered as fluctuations of F'_σ and \bar{F}'_σ around $O(N)$ singlet fields $\sum_{i=1}^N \phi_i(x) \psi_{\sigma i}(x)/N$ and $\sum_{i=1}^N \phi_i^*(x) \bar{\psi}_{\sigma i}(x)/N$ respectively, both of which are arithmetic averages of many fields in terms of the large N . As we will see below we can in principle control these fluctuations by changing N itself. The partition function Eq.(3) then becomes

$$\begin{aligned} Z &= c \int \mathcal{D}[\bar{F}'_\sigma, F'_\sigma] \mathcal{D}[\phi_i^*, \phi_i] \mathcal{D}[\bar{\psi}_{\sigma i}, \psi_{\sigma i}] \\ &\quad \exp \left\{ \int dx dy \left[\sum_{i=1}^N \phi_i^*(x) D^{-1}(x, y) \phi_i(y) + \sum_{i=1}^N \sum_{\sigma=\uparrow,\downarrow} \bar{\psi}_{\sigma i}(x) S^{-1}(x, y) \psi_{\sigma i}(y) \right] \right. \\ &\quad \left. - \int dx \left[\sum_{i,j=1}^N \sum_{\sigma=\uparrow,\downarrow} \frac{g_{bf}}{N} \phi_i^*(x) \bar{\psi}_{\sigma i}(x) \phi_j(x) \psi_{\sigma j}(x) - \frac{N}{g_{bf}} \sum_{\sigma=\uparrow,\downarrow} \bar{F}'_\sigma(x) F'_\sigma(x) \right] \right\} \\ &= c \int \mathcal{D}[\bar{F}_\sigma, F_\sigma] \mathcal{D}[\phi_i^*, \phi_i] \mathcal{D}[\bar{\psi}_{\sigma i}, \psi_{\sigma i}] \\ &\quad \exp \left\{ \int dx dy \left[\sum_{i=1}^N \phi_i^*(x) D^{-1}(x, y) \phi_i(y) + \sum_{i=1}^N \sum_{\sigma=\uparrow,\downarrow} \bar{\psi}_{\sigma i}(x) S^{-1}(x, y) \psi_{\sigma i}(y) \right] \right. \\ &\quad \left. + \int dx \sum_{\sigma=\uparrow,\downarrow} \left[\frac{N}{g_{bf}} \bar{F}_\sigma(x) F_\sigma(x) + \sum_{i=1}^N \bar{F}_\sigma(x) \phi_i(x) \psi_{\sigma i}(x) + \sum_{i=1}^N \phi_i^*(x) \bar{\psi}_{\sigma i}(x) F_\sigma(x) \right] \right\}, \quad (8) \end{aligned}$$

where $D^{-1}(x, y)$ and $S^{-1}(x, y)$ denote inverse Green's functions of bosons and fermions, respectively:

$$D^{-1}(x, y) = \left(-\partial_\tau + \frac{\nabla^2}{2m_b} + \mu_b \right) \delta(x - y), \quad (9)$$

$$S^{-1}(x, y) = \left(-\partial_\tau + \frac{\nabla^2}{2m_f} + \mu_f \right) \delta(x - y). \quad (10)$$

We also used a simple notation for functional integral measures:

$$\mathcal{D}[\bar{F}_\sigma, F_\sigma] \mathcal{D}[\phi_i^*, \phi_i] \mathcal{D}[\bar{\psi}_{\sigma i}, \psi_{\sigma i}] = \left(\prod_{\sigma=\uparrow,\downarrow} \mathcal{D}\bar{F}_\sigma \mathcal{D}F_\sigma \right) \left(\prod_{i=1}^N \mathcal{D}\phi_i^* \mathcal{D}\phi_i \right) \left(\prod_{i=1}^N \prod_{\sigma=\uparrow,\downarrow} \mathcal{D}\bar{\psi}_{\sigma i} \mathcal{D}\psi_{\sigma i} \right). \quad (11)$$

Note that as in a usual Hubbard-Stratonovich transformation the introduction of auxiliary fields reduces the original bosonic and fermionic fields into bilinear forms which are diagonalized in terms of the large N indices, and they can be integrated out immediately. We first perform the fermionic functional integral in Eq.(8), and the relevant part of the integration yields for each pair of indices $\sigma = \uparrow, \downarrow$ and $i = 1, \dots, N$ (*i.e.*, summation over σ and i is not assumed here),

$$\begin{aligned}
& \int \mathcal{D}\bar{\psi}_{\sigma i} \mathcal{D}\psi_{\sigma i} \exp \left\{ \int dx dy [\bar{\psi}_{\sigma i}(x) S^{-1}(x, y) \psi_{\sigma i}(y) + \bar{F}_{\sigma}(x) \phi_i(x) \delta(x - y) \psi_{\sigma i}(y) + \phi_i^*(x) \delta(x - y) \bar{\psi}_{\sigma i}(y) F_{\sigma}(y)] \right\} \\
&= \int \mathcal{D}\bar{\psi}_{\sigma i} \mathcal{D}\psi_{\sigma i} \exp \left\{ \int dx dy [\bar{\psi}_{\sigma i}(x) + \int dz \bar{F}_{\sigma}(z) \phi_i(z) S(z, x)] S^{-1}(x, y) [\psi_{\sigma i}(y) + \int dw S(y, w) \phi_i^*(w) F_{\sigma}(w)] \right. \\
&\quad \left. - \int dx dy dz dw \bar{F}_{\sigma}(z) \phi_i(z) S(z, x) S^{-1}(x, y) S(y, w) \phi_i^*(w) F_{\sigma}(w) \right\} \\
&= \int \mathcal{D}\bar{\psi}'_{\sigma i} \mathcal{D}\psi'_{\sigma i} \exp \left\{ \int dx dy \bar{\psi}'_{\sigma i}(x) S^{-1}(x, y) \psi'_{\sigma i}(y) \right\} \exp \left\{ - \int dz dw \bar{F}_{\sigma}(z) \phi_i(z) S(z, w) \phi_i^*(w) F_{\sigma}(w) \right\} \\
&= \exp \left\{ \ln \det [-S^{-1}(x, y)] - \int dx dy \phi_i^*(x) \bar{F}_{\sigma}(y) S(y, x) F_{\sigma}(x) \phi_i(y) \right\} \\
&= \exp \left\{ \text{tr} \ln [-S^{-1}(x, y)] - \int dx dy \phi_i^*(x) A_{\sigma}(x, y) \phi_i(y) \right\}, \tag{12}
\end{aligned}$$

where “tr” and “det” are taken only over coordinate indices, and $A_{\sigma}(x, y)$ is defined by $A_{\sigma}(x, y) = \bar{F}_{\sigma}(y) S(y, x) F_{\sigma}(x)$, whose ordering is important due to the anti-commuting nature of Grassmann fields \bar{F}_{σ} and F_{σ} . We have also used a matrix formula: $\ln \det M = \text{tr} \ln M$. Thus, Eq.(8) reduces to

$$\begin{aligned}
Z &= c [Z_0^f(\mu_f)]^N \int \mathcal{D}[\bar{F}_{\sigma}, F_{\sigma}] \mathcal{D}[\phi_i^*, \phi_i] \tag{13} \\
&\exp \left\{ \int dx dy \sum_{i=1}^N \phi_i^*(x) \left[D^{-1}(x, y) - \sum_{\sigma=\uparrow, \downarrow} A_{\sigma}(x, y) \right] \phi_i(y) + \frac{N}{g_{bf}} \int dx \sum_{\sigma=\uparrow, \downarrow} \bar{F}_{\sigma}(x) F_{\sigma}(x) \right\},
\end{aligned}$$

with a partition function for a two-component free Fermi gas $Z_0^f(\mu_f) = \exp\{2\text{tr} \ln [-S^{-1}(x, y)]\}$. We proceed to perform bosonic functional integral, and the relevant part of the integration yields for each index $i = 1, \dots, N$,

$$\begin{aligned}
& \int \mathcal{D}\phi_i^* \mathcal{D}\phi_i \exp \left\{ \int dx dy \phi_i^*(x) \left[D^{-1}(x, y) - \sum_{\sigma=\uparrow, \downarrow} A_{\sigma}(x, y) \right] \phi_i(y) \right\} \\
&= \left\{ \det \left[-D^{-1}(x, y) + \sum_{\sigma=\uparrow, \downarrow} A_{\sigma}(x, y) \right] \right\}^{-1} \\
&= \left\{ \det \int dz [-D^{-1}(x, z)] \left[\delta(z - y) - \sum_{\sigma=\uparrow, \downarrow} \int dw D(z, w) A_{\sigma}(w, y) \right] \right\}^{-1} \\
&= \exp \left\{ -\text{tr} \ln [-D^{-1}(x, y)] - \text{tr} \ln \left[\delta(x - y) - \sum_{\sigma=\uparrow, \downarrow} \int dw D(x, w) A_{\sigma}(w, y) \right] \right\}. \tag{14}
\end{aligned}$$

Applying Eq.(14) to Eq.(13), we obtain a partition function which is described only by CF fields:

$$Z = c[Z_0^b(\mu_b)Z_0^f(\mu_f)]^N \times \int \mathcal{D}[\bar{F}_\sigma, F_\sigma] \exp\left\{\frac{N}{g_{bf}} \int dx \sum_{\sigma=\uparrow,\downarrow} \bar{F}_\sigma(x)F_\sigma(x) - N \text{tr} \ln \left[\delta(x-y) - \sum_{\sigma=\uparrow,\downarrow} \int dw D(x,w)A_\sigma(w,y) \right]\right\}, \quad (15)$$

with a partition function for the ideal Bose gas $Z_0^b(\mu_b) = \exp\{-\text{tr} \ln[-D^{-1}(x,y)]\}$. The corresponding action becomes

$$S[\bar{F}_\sigma, F_\sigma] = -\frac{N}{g_{bf}} \int dx \sum_{\sigma=\uparrow,\downarrow} \bar{F}_\sigma(x)F_\sigma(x) + N \text{tr} \ln \left[\delta(x-y) - \sum_{\sigma=\uparrow,\downarrow} \int dw D(x,w)A_\sigma(w,y) \right]. \quad (16)$$

Since N becomes an overall factor in the action and plays the same role as \hbar in a usual loop expansion, our $1/N$ -expansion is equivalent to the loop expansion based on the CF action Eq.(16)¹. Let us normalize the CF fields as

$$\mathcal{F}_\sigma(x) = \sqrt{N}F_\sigma(x), \quad (17)$$

$$\bar{\mathcal{F}}_\sigma(x) = \sqrt{N}\bar{F}_\sigma(x), \quad (18)$$

$$\mathcal{A}_\sigma(x,y) = \bar{\mathcal{F}}_\sigma(y)S(y,x)\mathcal{F}_\sigma(x) = NA_\sigma(x,y), \quad (19)$$

which give an explicit form of the $1/N$ -expansion, with the use of a formula in the logarithm: $\ln(1 - M) = -\sum_{k=1}^{\infty} M^k/k$,

$$\begin{aligned} S[\bar{F}_\sigma, F_\sigma] &= -\frac{1}{g_{bf}} \int dx \sum_{\sigma=\uparrow,\downarrow} \bar{\mathcal{F}}_\sigma(x)\mathcal{F}_\sigma(x) + N \text{tr} \ln \left[\delta(x-y) - \frac{1}{N} \int dw \sum_{\sigma=\uparrow,\downarrow} D(x,w)\mathcal{A}_\sigma(w,y) \right] \\ &= -\frac{1}{g_{bf}} \int dx \sum_{\sigma=\uparrow,\downarrow} \bar{\mathcal{F}}_\sigma(x)\mathcal{F}_\sigma(x) - \sum_{k=1}^{\infty} \left(\frac{1}{N}\right)^{k-1} \frac{1}{k} \text{tr} \left\{ \int dw \sum_{\sigma=\uparrow,\downarrow} D(x,w)\bar{\mathcal{F}}_\sigma(y)S(y,w)\mathcal{F}_\sigma(w) \right\}^k \\ &=: \mathcal{S}[\bar{\mathcal{F}}_\sigma, \mathcal{F}_\sigma]. \end{aligned} \quad (20)$$

Here one can see that there is no internal degree of freedom associated with the large N extension and that $1/N$ only appears as a suppression factor of each higher-dimensional interaction between CFs. Then, we reach the following representation of the partition,

$$Z = c'[Z_0^b(\mu_b)Z_0^f(\mu_f)]^N \int \mathcal{D}[\bar{\mathcal{F}}_\sigma, \mathcal{F}_\sigma] \exp\{-\mathcal{S}[\bar{\mathcal{F}}_\sigma, \mathcal{F}_\sigma]\}, \quad (21)$$

with a normalization constant c' . Figure 2 shows a formal expression of the CF action $\mathcal{S}[\bar{\mathcal{F}}_\sigma, \mathcal{F}_\sigma]$ of Eq.(20) in terms of Feynman graphs. We will give precise definitions of Σ (“self-energy”), Γ_4 (4-point

¹In general when we have an overall factor $1/r$ in our action, propagators should be proportional to r , while any kind of vertices to $1/r$. Then, any graph composed of P propagators and V vertices is proportional to r^{P-V} . On the other hand, such a graph has $L = P - (V - 1)$ loops, which yields a relation: $r^{P-V} = r^{L-1}$. Therefore, the series expansion in terms of r is equivalent to the loop expansion in diagrammatic expressions [22]. Setting $1/r = N$ yields our $1/N$ -expansion.

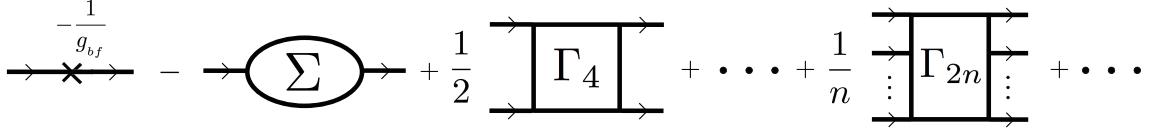


Figure 2: Graphical representation of the CF action $\mathcal{S}[\bar{\mathcal{F}}_\sigma, \mathcal{F}_\sigma]$ in Eq.(20). The thick lines represent the external lines of CF fields $\bar{\mathcal{F}}_\sigma$ and \mathcal{F}_σ . Definitions of Σ , Γ_4 and Γ_{2n} will be given later in Eq.(25), (48) and (67), respectively.

vertex function) and Γ_{2n} ($2n$ -point vertex function) later in Eq.(25), (48) and (67), respectively. It will be shown that the first two graphs in Fig.2 yields an inverse propagator of CFs which behaves as a free Fermi particle within our approximation, and the rest of graphs can be considered as interaction vertices of CFs.

4 $1/N$ -expansion of strongly-coupled boson-fermion mixtures

In the following, we will perform the $1/N$ -expansion based on Eq.(20) up to the next-to-leading-order terms and derive a low-energy effective theory of CFs. We will show that under an assumption discussed below an effective interaction between CFs are weakly attractive, and that the BCS-superfluidity of CFs (CF-BCS) is realized at sufficiently low temperatures.

4.1 The leading-order terms

The leading-order (LO) terms in the $1/N$ -expansion, *i.e.*, $O(1)$ terms in Eq.(20), become

$$\mathcal{S}_{\text{LO}}[\bar{\mathcal{F}}_\sigma, \mathcal{F}_\sigma] = -\frac{1}{g_{bf}} \int dx \sum_{\sigma=\uparrow, \downarrow} \bar{\mathcal{F}}_\sigma(x) \mathcal{F}_\sigma(x) - \int dx dw \sum_{\sigma=\uparrow, \downarrow} \bar{\mathcal{F}}_\sigma(x) D(x, w) S(x, w) \mathcal{F}_\sigma(w), \quad (22)$$

which we can rewrite with the use of Fourier transforms (see Appendix A) as,

$$\begin{aligned} \mathcal{S}_{\text{LO}}[\bar{\mathcal{F}}_\sigma, \mathcal{F}_\sigma] &= -\frac{1}{g_{bf}} \int dp \sum_{\sigma=\uparrow, \downarrow} \bar{\mathcal{F}}_\sigma(p) \mathcal{F}_\sigma(p) - \int dp \sum_{\sigma=\uparrow, \downarrow} \bar{\mathcal{F}}_\sigma(p) \left[\int dq D(q) S(p-q) \right] \mathcal{F}_\sigma(p) \\ &= -\int dp \sum_{\sigma=\uparrow, \downarrow} \bar{\mathcal{F}}_\sigma(p) G^{-1}(p) \mathcal{F}_\sigma(p). \end{aligned} \quad (23)$$

Here we have used notations: $p = (\mathbf{p}, i\omega)$, $\int dp = T \sum_\omega \int d\mathbf{p} / (2\pi)^3$ with the Matsubara frequency ω and spatial momentum vector \mathbf{p} . Also, we have introduced an inverse propagator of CF fields \mathcal{F}_σ as

$$G^{-1}(p) = \frac{1}{g_{bf}} + \Sigma(p), \quad (24)$$

with a CF “self-energy”, or single “bubble” of bosons and fermions, $\Sigma(p)$ given by

$$\Sigma(p) = \int dq D(q) S(p-q). \quad (25)$$

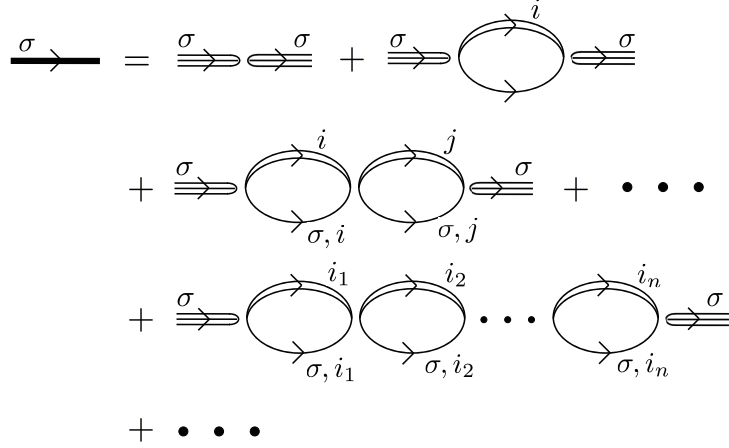


Figure 3: Graphical representation of the propagator for “bare” CF fields F_σ (not for \mathcal{F}_σ). In the right hand side, the external triple line denotes a pair of single boson and fermion, and only appears as a shorthand notation for a half of the vertex in Fig. 1(c). As for the propagator of \mathcal{F}_σ ($:= \sqrt{N}F_\sigma$) fields, we need to multiply both sides by the normalization factor N .

Equations (24) and (25) show that the propagator is represented by an infinite geometric series of the original boson-fermion bubbles, as shown in Fig. 3. In the right hand side of Fig. 3, we can see that the n -th graph has large N power-counting factors (i) N^{n-1} from $n-1$ internal loops, (ii) $(1/N)^n$ from n vertices, and (iii) $(\sqrt{N})^2$ from the normalization ($\mathcal{F}_\sigma = \sqrt{N}F_\sigma$) for any $n \in \mathbb{N}$, which give an $O(1/N^0)$ term in total, *i.e.*, the leading-order contribution in the $1/N$ -expansion as shown in Eqs.(23)-(25).

Let us expand the inverse propagator G^{-1} in order to derive a low-energy effective theory of CFs. The summation over the bosonic Matsubara frequency in the self-energy Eq.(25) is performed as

$$\begin{aligned}
\Sigma(p) &= \int dq D(q) S(p-q) \\
&= T \sum_{\omega_b} \int \frac{d\mathbf{q}}{(2\pi)^3} \frac{1}{i\omega_b - \xi_b(\mathbf{q})} \frac{1}{i(\omega - \omega_b) - \xi_f(\mathbf{p} - \mathbf{q})} \\
&= \int \frac{d\mathbf{q}}{(2\pi)^3} \lim_{\eta \downarrow 0} \frac{1}{2\pi i} \oint_C dz \frac{e^{\eta z}}{e^{\beta z} - 1} \frac{1}{z - \xi_b(\mathbf{q})} \frac{1}{i\omega - z - \xi_f(\mathbf{p} - \mathbf{q})} \\
&= \int \frac{d\mathbf{q}}{(2\pi)^3} \frac{1 - n_f(\mathbf{p} - \mathbf{q}) + n_b(\mathbf{q})}{\xi_f(\mathbf{p} - \mathbf{q}) + \xi_b(\mathbf{q}) - i\omega}, \tag{26}
\end{aligned}$$

where $n_b(\mathbf{k})$ and $n_f(\mathbf{k})$ denote the Bose-Einstein and Fermi-Dirac distribution functions, respectively,

$$n_b(\mathbf{k}) = \frac{1}{e^{\beta \xi_b(\mathbf{k})} - 1}, \tag{27}$$

$$n_f(\mathbf{k}) = \frac{1}{e^{\beta \xi_f(\mathbf{k})} + 1}, \tag{28}$$

with ξ_b and ξ_f kinetic energies of single boson and fermion relative to the chemical potentials μ_b and μ_f , respectively: $\xi_b(\mathbf{k}) = \mathbf{k}^2/2m_b - \mu_b$, $\xi_f(\mathbf{k}) = \mathbf{k}^2/2m_f - \mu_f$. Here we have taken a standard contour

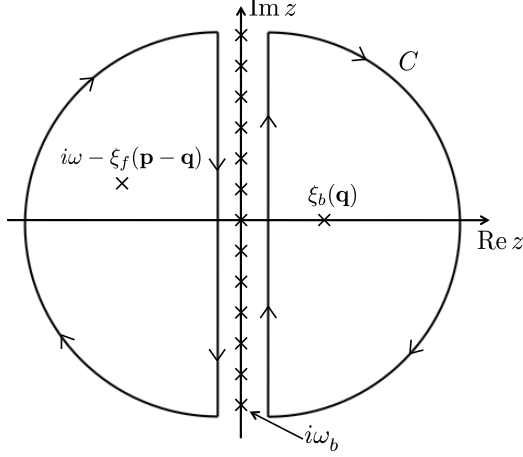


Figure 4: Contour for evaluation of the Matsubara frequency sum in Eq.(26). The crosses indicate the position of the poles in the integrand.

C on the complex z -plane (see Fig. 4) in order to convert the summation over the bosonic Matsubara frequency ω_b into a complex-integration along C [22]. Then the inverse propagator Eq.(24) reads

$$G^{-1}(p) = \frac{m_R}{2\pi a_{bf}} - \int \frac{d\mathbf{q}}{(2\pi)^3} \left\{ \frac{1}{\varepsilon(\mathbf{q})} - \frac{1 - n_f(\mathbf{p} - \mathbf{q}) + n_b(\mathbf{q})}{\xi_f(\mathbf{p} - \mathbf{q}) + \xi_b(\mathbf{q}) - i\omega} \right\}, \quad (29)$$

where the kinetic energy in the relative coordinate $\varepsilon(\mathbf{q})$ is defined by $\varepsilon(\mathbf{q}) = \mathbf{q}^2/(2m_R)$, and by using Eq.(2) we replaced the coupling constant g_{bf} with the scattering length a_{bf} . Note that up to this stage there is no need to put any assumption related to the strength of our coupling constant g_{bf} , or $n_{\text{tot}}^{1/3} a_{bf}$.

Now let us study a strongly-coupled mixture characterized by $0 \leq n_{\text{tot}}^{1/3} a_{bf} \ll 1$. In this case, it is natural to consider the situation that both μ_b and μ_f are almost equal to $-\omega_{bf}/2$, where ω_{bf} is a binding energy of an isolated boson-fermion pair in the vacuum: $\omega_{bf} = 1/(2m_R a_{bf}^2)$. This is in accordance with the fact that in the strongly-coupled mixture the system becomes a dilute gas of CFs due to $n_{\text{tot}}^{1/3} |a_{bf}| \ll 1$. We will later see that the number equations to relate the chemical potentials and the particle density indeed have a solution $\mu_b + \mu_f \simeq -\omega_{bf}$. This implies putting one more pair reduces the total energy by an energy almost equal to ω_{bf} .

Then, the low energy and low momentum expansions of Eq.(29) at zero temperature gives (see Appendix B)

$$G^{-1}(\mathbf{p}, E) \simeq \frac{m_R}{2\pi a_{bf}} - \frac{(2m_R)^{3/2}}{4\pi} \sqrt{|\mu| + \frac{\mathbf{p}^2}{2(m_b + m_f)} - E}, \quad (30)$$

where μ denotes a total boson-fermion chemical potential: $\mu = \mu_f + \mu_b (< 0)$, and the chemical potentials are yet to be determined. We proceed to expand Eq.(30) in terms of $\{\mathbf{p}^2/[2(m_b + m_f)] -$

$E\}/|\mu|$, to obtain the derivative expansion of the inverse propagator,

$$G^{-1}(\mathbf{p}, E) \simeq a - c \mathbf{p}^2 + d E, \quad (31)$$

with the zero temperature coefficients

$$a = \frac{m_R}{2\pi a_{bf}} - \frac{m_R \sqrt{2m_R |\mu|}}{2\pi}, \quad (32)$$

$$c = \frac{1}{4\pi} \frac{m_R}{m_f + m_b} \sqrt{\frac{m_R}{2|\mu|}}, \quad (33)$$

$$d = \frac{m_R}{2\pi} \sqrt{\frac{m_R}{2|\mu|}}. \quad (34)$$

Thus in low-energy scales, Eq.(23) can be approximated by its effective action,

$$\mathcal{S}_{\text{LO}}[\bar{\mathcal{F}}_\sigma, \mathcal{F}_\sigma] \simeq - \int dp \sum_{\sigma=\uparrow, \downarrow} \sqrt{d} \bar{\mathcal{F}}_\sigma(p) \left(i\omega - \frac{\mathbf{p}^2}{2[d/(2c)]} + \frac{a}{d} \right) \sqrt{d} \mathcal{F}_\sigma(p). \quad (35)$$

Performing a proper normalization of CF fields with $\Psi_\sigma = \sqrt{d} \mathcal{F}_\sigma$, $\bar{\Psi}_\sigma = \sqrt{d} \bar{\mathcal{F}}_\sigma$ yields a low-energy effective action,

$$\mathcal{S}_{\text{LO}}^{\text{eff.}}[\bar{\Psi}_\sigma, \Psi_\sigma] = - \int dp \sum_{\sigma=\uparrow, \downarrow} \bar{\Psi}_\sigma(p) \left(i\omega - \frac{\mathbf{p}^2}{2m_{\text{F}}} + \mu_{\text{F}} \right) \Psi_\sigma(p), \quad (36)$$

with the kinetic mass $m_{\text{F}} = d/(2c)$ and the chemical potential $\mu_{\text{F}} = a/d$ for the normalized CF fields $\Psi_\sigma, \bar{\Psi}_\sigma$:

$$m_{\text{F}} = m_f + m_b, \quad (37)$$

$$\mu_{\text{F}} = 2\omega_{bf} (\sqrt{X} - X). \quad (38)$$

Here we have defined a dimensionless parameter $X = |\mu|/\omega_{bf}$. Using the effective action Eq.(36), we can construct an effective theory described by the following partition function,

$$Z_{\text{LO}}^{\text{eff.}} = c [Z_0^b(\mu_b) Z_0^f(\mu_f)]^N \int \left(\prod_{\sigma=\uparrow, \downarrow} \mathcal{D}\bar{\Psi}_\sigma \mathcal{D}\Psi_\sigma \right) \exp\{-\mathcal{S}_{\text{LO}}^{\text{eff.}}[\bar{\Psi}_\sigma, \Psi_\sigma]\}, \quad (39)$$

which is valid for phenomena dominated by low-energy and low-momentum scales such that $\omega/|\mu| \ll 1$, $\varepsilon(\mathbf{p})/|\mu| \ll 1$, and the chemical potential $|\mu|$ is determined by number equations,

$$n_{\text{tot}} = - \frac{\partial}{\partial \mu_b} \ln Z = - \frac{\partial}{\partial \mu_f} \ln Z. \quad (40)$$

We will estimate chemical potentials, μ_f , μ_b and μ_{F} , at zero temperature, where the number

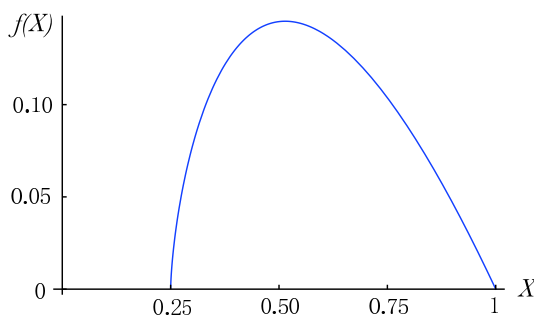


Figure 5: Numerical plot of $f(X) = (\sqrt{X} - X)(2 - 1/\sqrt{X})^{2/3}$ as a function of X .

equations reduce to

$$\begin{aligned}
n_{\text{tot}} &= -\frac{\partial}{\partial \mu_b} \ln Z \\
&= -\frac{\partial}{\partial \mu_b} \ln Z_{\text{LO}}^{\text{eff.}} - N \frac{\partial}{\partial \mu_b} \ln Z_0^b(\mu_b) \\
&= -\left(\frac{\partial}{\partial \mu_F} \ln Z_{\text{LO}}^{\text{eff.}}\right) \times \left(\frac{\partial \mu_F}{\partial \mu_b}\right) + N \int \frac{d\mathbf{k}}{(2\pi)^3} n_b(\mathbf{k}) \\
&= \frac{(2m_F \mu_F)^{3/2}}{3\pi^2} \times \left(2 - \frac{1}{\sqrt{X}}\right). \tag{41}
\end{aligned}$$

Here we used the fact that $n_b(\mathbf{k})$ vanishes at $T = 0$ with $\mu_b < 0$ and also that the effective action Eq.(36) is the same action as for a two-component free Fermi gas with a mass m_F and a chemical potential μ_F . We can rewrite Eq.(41) as a dimensionless equation,

$$\begin{aligned}
\frac{(3\pi^2)^{2/3}}{2} \left(\frac{m_R}{m_F}\right) (n_{\text{tot}}^{1/3} a_{bf})^2 &= (\sqrt{X} - X) \left(2 - \frac{1}{\sqrt{X}}\right)^{2/3} \\
&=: f(X), \tag{42}
\end{aligned}$$

where we defined a function f as $f(X) = (\sqrt{X} - X)(2 - 1/\sqrt{X})^{2/3}$. Figure 5 shows a numerical plot of $f(X)$ as a function of X , and we can see that $f(X)$ becomes zero at $X = 1/4$ and $X = 1$. Since the left hand side of Eq.(42) becomes quite small in the strongly-coupled mixture, Eq.(42) will give two solutions around $X \sim 1/4$ and $X \sim 1$. From now on, we will focus on a solution $X \sim 1$ which is consistent with the case of the dilute gas as we have mentioned before.

Based on the above argument, we introduce a small positive parameter $\delta (= 1 - X)$ which should be determined through the number equations. Putting this into Eq.(41) yields

$$\begin{aligned}
\frac{(3\pi^2 n_{\text{tot}})^{2/3}}{2m_F} &= \mu_F \times \left(2 - \frac{1}{\sqrt{X}}\right)^{2/3} \\
&\simeq \omega_{bf} \delta, \tag{43}
\end{aligned}$$

which finally gives

$$|\mu| = \omega_{bf} - \epsilon_F + O(\epsilon_F/\omega_{bf}), \quad (44)$$

$$\mu_F = \epsilon_F + O(\epsilon_F/\omega_{bf}), \quad (45)$$

with a Fermi energy of CFs $\epsilon_F = (3\pi^2 n_{\text{tot}})^{2/3}/(2m_F)$. Note that the above analysis becomes reliable only with a small $\delta (\simeq \epsilon_F/\omega_{bf})$ which demands the following condition:

$$\frac{\epsilon_F}{\omega_{bf}} = \frac{(3\pi^2)^{2/3} n_{\text{tot}}^{2/3}}{2m_F} \times \left(\frac{1}{2m_R a_{bf}^2} \right)^{-1} = (3\pi^2)^{2/3} \left(\frac{m_R}{m_F} \right) (n_{\text{tot}}^{1/3} a_{bf})^2 \ll 1. \quad (46)$$

Now we can see that Eq.(46) is automatically satisfied in our strongly-coupled mixture such that $0 \leq n_{\text{tot}}^{1/3} a_{bf} \ll 1$.

Combining Eqs.(36) and (45), we find that in the leading order of the $1/N$ -expansion a low-energy effective theory of the strongly-coupled boson-fermion mixture, whose energy scales satisfy $T/\omega_{bf} \ll 1$, $\omega/\omega_{bf} \ll 1$ and $\varepsilon(\mathbf{p})/\omega_{bf} \ll 1$, becomes just a two-component free Fermi gas of CFs with a mass $m_F = m_b + m_f$ and the same number density as the total number density of the original fermions n_{tot} . We remark that in our strongly-coupled mixture the small expansion parameters are $1/N$ and $n_{\text{tot}}^{1/3} a_{bf}$.

4.2 The next-to-leading-order term

We proceed to study the next-to-leading-order (NLO) term in Eq.(20), and we will show that the NLO term gives an effective attraction between CFs in low-energy scales. The NLO term in Eq.(20) becomes

$$\begin{aligned} & \mathcal{S}_{\text{NLO}}[\bar{\mathcal{F}}_\sigma, \mathcal{F}_\sigma] \\ &= -\frac{1}{2N} \text{tr} \int dv dw dz \sum_{\sigma, \rho = \uparrow, \downarrow} D(x, w) \mathcal{A}_\sigma(w, v) D(v, z) \mathcal{A}_\rho(z, y) \\ &= -\frac{1}{2N} \sum_{\sigma, \rho = \uparrow, \downarrow} \int dx dv dw dz D(x, w) \bar{\mathcal{F}}_\sigma(v) S(v, w) \mathcal{F}_\sigma(w) D(v, z) \bar{\mathcal{F}}_\rho(x) S(x, z) \mathcal{F}_\rho(z) \\ &= -\frac{1}{2N} \sum_{\sigma, \rho = \uparrow, \downarrow} \int \left(\prod_{i=1}^4 dp_i \right) \delta(p_4 + p_2 - p_1 - p_3) \\ & \quad \times \left[\int dq D(q) S(p_2 - q) D(p_1 - p_2 + q) S(p_3 - q) \right] \bar{\mathcal{F}}_\sigma(p_1) \bar{\mathcal{F}}_\rho(p_3) \mathcal{F}_\rho(p_4) \mathcal{F}_\sigma(p_2) \\ &= \frac{1}{2} \sum_{\sigma, \rho = \uparrow, \downarrow} \int \left(\prod_{i=1}^4 dp_i \right) \delta(p_4 + p_2 - p_1 - p_3) \Gamma_4(\{p_i\}_{i=1}^4) \bar{\mathcal{F}}_\sigma(p_1) \bar{\mathcal{F}}_\rho(p_3) \mathcal{F}_\rho(p_4) \mathcal{F}_\sigma(p_2), \quad (47) \end{aligned}$$

where Γ_4 represents the proper 4-point vertex of CFs, defined by

$$\Gamma_4(\{p_i\}_{i=1}^4) = -\frac{1}{N} \int dq D(q) S(p_2 - q) D(p_1 - p_2 + q) S(p_3 - q), \quad (48)$$

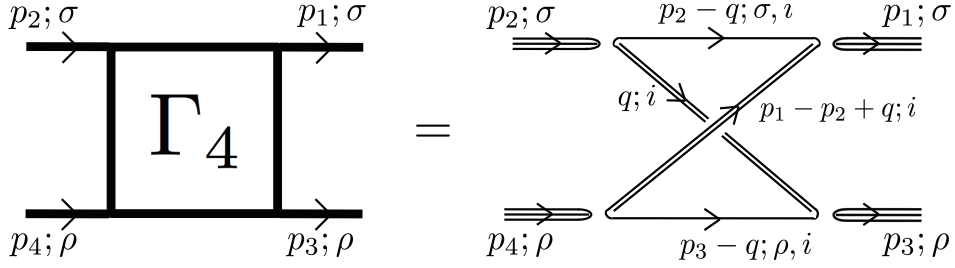


Figure 6: Graphical representation of the proper 4-point vertex of “bare” CF fields F_σ (again, not for \mathcal{F}_σ). In order to obtain the proper 4-point vertex of \mathcal{F}_σ , we need to multiply both sides by $(\sqrt{N})^4$, which comes from the normalization of four external legs ($\mathcal{F}_\sigma = \sqrt{N}F_\sigma$).

with a set of momenta $\{p_i\}_{i=1}^4 = \{p_1, p_2, p_3, p_4\}$ constrained by the energy-momentum conservation, $p_4 + p_2 - p_1 - p_3 = 0$. The graphical representation of Eq.(48) is shown in Fig. 6, which indicates that the CFs interact through the exchange of their constituent particles. We can see that the right hand side of Fig. 6 gives large N power-counting factors (i) N from an internal loop, (ii) $(1/N)^4$ from four vertices, and (iii) $(\sqrt{N})^4$ from the normalization ($\mathcal{F}_\sigma = \sqrt{N}F_\sigma$), which yield an $O(1/N)$ term as is Γ_4 in Eq.(48).

For a low-energy effective theory, we expand the proper 4-point vertex in terms of E/ω_{bf} with a small energy scale E relative to its binding energy ω_{bf} . Then the dominant contribution becomes

$$\Gamma_4(\{p_i\}) = \Gamma_4(\{(\mathbf{0}, \pi T), (\mathbf{0}, \pi T), (\mathbf{0}, -\pi T), (\mathbf{0}, -\pi T)\}) + O(E/\omega_{bf}). \quad (49)$$

We note that at finite temperatures it is impossible to put the frequencies in Γ_4 equal to zero, since the CF fields in Eq.(47) are Grassmann fields (purely fermionic) and do not have Matsubara zero mode, *i.e.*, $\omega = (2n + 1)\pi T$, $n \in \mathbb{Z}$. Note also that our procedure is essentially the same as in the derivation of the effective theory for Cooper pairs, which can be considered as composite bosons in two-component Fermi gases [16–18, 23–26]. Let us denote the low-energy effective vertex in Eq.(49) by $\Gamma_4(0)$, which becomes

$$\begin{aligned} \Gamma_4(0) &= \Gamma_4(\{(\mathbf{0}, \pi T), (\mathbf{0}, \pi T), (\mathbf{0}, -\pi T), (\mathbf{0}, -\pi T)\}) \\ &= -\frac{1}{N} T \sum_{\omega_b} \int \frac{d\mathbf{q}}{(2\pi)^3} D(\mathbf{q}, \omega_b) S(-\mathbf{q}, \pi T - \omega_b) D(\mathbf{q}, \omega_b) S(-\mathbf{q}, -\pi T - \omega_b) \\ &= -\frac{1}{N} \int \frac{d\mathbf{q}}{(2\pi)^3} T \sum_{\omega_b} \frac{1}{i\pi T - i\omega_b - \xi_f(-\mathbf{q})} \frac{1}{-i\pi T - i\omega_b - \xi_f(-\mathbf{q})} \left(\frac{1}{i\omega_b - \xi_b(\mathbf{q})} \right)^2. \quad (50) \end{aligned}$$

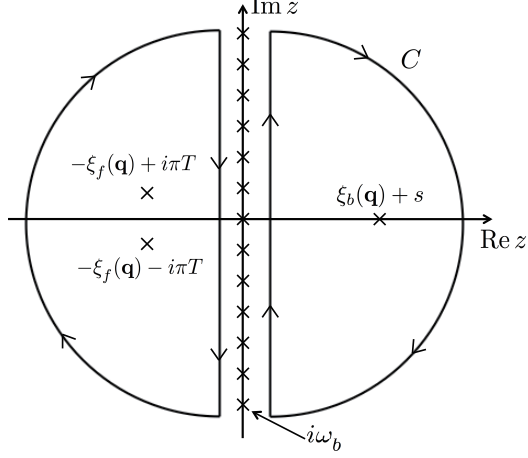


Figure 7: Contour for evaluation of the Matsubara frequency sum in Eq.(51). The crosses indicate the position of the poles in the integrand.

We can perform the summation over the bosonic Matsubara frequency ω_b in Eq.(50) as follows,

$$\begin{aligned}
& T \sum_{\omega_b} \frac{1}{i\pi T - i\omega_b - \xi_f(-\mathbf{q})} \frac{1}{-i\pi T - i\omega_b - \xi_f(-\mathbf{q})} \left(\frac{1}{i\omega_b - \xi_b(\mathbf{q})} \right)^2 \\
&= \lim_{\eta \downarrow 0} \frac{1}{2\pi i} \oint_C dz \frac{e^{\eta z}}{e^{\beta z} - 1} \frac{1}{z - i\pi T + \xi_f(\mathbf{q})} \frac{1}{z + i\pi T + \xi_f(\mathbf{q})} \frac{\partial}{\partial s} \left(\frac{1}{z - \xi_b(\mathbf{q}) - s} \right) \Big|_{s=0} \\
&= [1 - n_f(\mathbf{q}) + n_b(\mathbf{q})] \frac{2 [\xi_f(\mathbf{q}) + \xi_b(\mathbf{q})]}{\{[\xi_f(\mathbf{q}) + \xi_b(\mathbf{q})]^2 + (\pi T)^2\}^2} - \frac{1}{[\xi_f(\mathbf{q}) + \xi_b(\mathbf{q})]^2 + (\pi T)^2} \frac{\partial n_b(\mathbf{q})}{\partial \xi_b(\mathbf{q})}. \quad (51)
\end{aligned}$$

Here as in the calculation of Eq.(26), we have taken a standard contour C on the complex z -plane (see Fig. 7) in order to convert the Matsubara summation into a complex-integration along C . Substituting Eq.(51) into (50) yields

$$\begin{aligned}
\Gamma_4(0) &= -\frac{1}{N} \int \frac{d\mathbf{q}}{(2\pi)^3} \frac{2[\xi_f(\mathbf{q}) + \xi_b(\mathbf{q})] [1 - n_f(\mathbf{q}) + n_b(\mathbf{q})]}{\{[\xi_f(\mathbf{q}) + \xi_b(\mathbf{q})]^2 + (\pi T)^2\}^2} \\
&\quad + \frac{1}{N} \int \frac{d\mathbf{q}}{(2\pi)^3} \frac{1}{[\xi_f(\mathbf{q}) + \xi_b(\mathbf{q})]^2 + (\pi T)^2} \frac{\partial n_b(\mathbf{q})}{\partial \xi_b(\mathbf{q})}. \quad (52)
\end{aligned}$$

We will estimate $\Gamma_4(0)$ analytically at $T = 0$ with the same assumption as before, that is, with an assumption that both μ_b and μ_f are negative and their magnitudes are almost equal to $\omega_{b_f}/2$. This assumption still holds since the NLO term Eq.(47) is suppressed by a factor $1/N$ compared to the LO terms and does not change the values of chemical potentials so much from Eq.(44) and (45). Under

this assumption, $\Gamma_4(0)$ at $T = 0$ reduces to

$$\begin{aligned}
\Gamma_4(0) &= -\frac{1}{N} \int \frac{d\mathbf{q}}{(2\pi)^3} \frac{2}{[\xi_f(\mathbf{q}) + \xi_b(\mathbf{q})]^3} \\
&= -\frac{1}{N} \frac{(2m_R)^{3/2}}{\pi^2} \int_0^{\Lambda/\sqrt{2m_R}} \frac{x^2}{(x^2 + |\mu|)^3} dx \\
&= -\frac{1}{N} \frac{(2m_R)^{3/2}}{\pi^2} \frac{1}{8} \left\{ \frac{1}{|\mu|^{3/2}} \tan^{-1} \left(\frac{\Lambda}{\sqrt{2m_R}|\mu|} \right) + \frac{(\Lambda/\sqrt{2m_R})^3 - |\mu|\Lambda/(2m_R)}{|\mu| [|\mu| + \Lambda^2/(2m_R)]^2} \right\} \\
&\simeq -\frac{1}{N} \frac{1}{2\pi} \left(\frac{m_R}{2|\mu|} \right)^{3/2}, \tag{53}
\end{aligned}$$

where we have neglected $O(\sqrt{2m_R}|\mu|/\Lambda)$ corrections in the final step. Thus in low-energy scales, Eq.(47) can be approximated by

$$\begin{aligned}
\mathcal{S}_{\text{NLO}}[\bar{\mathcal{F}}_\sigma, \mathcal{F}_\sigma] \\
\simeq \frac{1}{2} \sum_{\sigma, \rho=\uparrow, \downarrow} \int \left(\prod_{i=1}^4 dp_i \right) \delta(p_4 + p_2 - p_1 - p_3) \Gamma_4(0) \bar{\mathcal{F}}_\sigma(p_1) \bar{\mathcal{F}}_\rho(p_3) \mathcal{F}_\rho(p_4) \mathcal{F}_\sigma(p_2). \tag{54}
\end{aligned}$$

According to the analysis on the LO terms, we perform the same normalization as in Eq.(36), $\Psi_\sigma = \sqrt{d}\mathcal{F}_\sigma$, $\bar{\Psi}_\sigma = \sqrt{d}\bar{\mathcal{F}}_\sigma$, which yields a low-energy effective action in the NLO,

$$\begin{aligned}
\mathcal{S}_{\text{NLO}}^{\text{eff.}}[\bar{\Psi}_\sigma, \Psi_\sigma] \\
= \frac{1}{2} \sum_{\sigma, \rho=\uparrow, \downarrow} \int \left(\prod_{i=1}^4 dp_i \right) \delta(p_4 + p_2 - p_1 - p_3) g_{\text{FF}} \bar{\Psi}_\sigma(p_1) \bar{\Psi}_\rho(p_3) \Psi_\rho(p_4) \Psi_\sigma(p_2). \tag{55}
\end{aligned}$$

Here we defined an effective four-Fermi coupling constant by $g_{\text{FF}} = \Gamma_4(0)/d^2$, which becomes

$$g_{\text{FF}} = -\frac{1}{N} \frac{2\pi a_{bf}}{m_R \sqrt{X}}. \tag{56}$$

We apply the LO result Eq.(44), *i.e.*, $X \simeq 1 - \varepsilon_F/\omega_{bf}$, to the above Eq.(56), and finally obtain

$$\begin{aligned}
g_{\text{FF}} &\simeq -\frac{1}{N} \frac{2\pi a_{bf}}{m_R} \left(1 + \frac{1}{2} \frac{\varepsilon_F}{\omega_{bf}} \right) \\
&\simeq -\frac{1}{N} \frac{2\pi a_{bf}}{m_R}. \tag{57}
\end{aligned}$$

Introducing the density of states per unit volume at the Fermi surface $N_F(0)$:

$$N_F(0) = \frac{m_F (3\pi^2 n_{\text{tot}})^{1/3}}{\pi^2}, \tag{58}$$

we have the dimensionless parameter for the strength of the effective four-Fermi interaction,

$$\begin{aligned}
N_F(0) g_{\text{FF}} &\simeq -\frac{m_F (3\pi^2 n_{\text{tot}})^{1/3}}{\pi^2} \frac{2\pi a_{bf}}{N m_R} \\
&= -2 \left(\frac{3}{\pi} \right)^{1/3} \frac{m_F}{m_R} \frac{n_{\text{tot}}^{1/3} a_{bf}}{N}. \tag{59}
\end{aligned}$$

Here we find that the NLO term yields an effective four-Fermi interaction, which is attractive and weak in a twofold meaning. First, we are considering strongly-coupled boson-fermion mixtures so that the dimensionless parameter $n_{\text{tot}}^{1/3} a_{bf}$ is positive and much smaller than 1, which makes $N_F(0)g_{\text{FF}}$ negative and much smaller than 1, as discussed in Ref. [7] for $N = 1$. Secondly, we also have large N degrees of freedom in the original boson-fermion mixture, which yield the large suppression factor $1/N$ in Eq.(59).

4.3 BCS superfluidity of composite fermions

From the results of the previous sections, we have a low-energy effective action up to the NLO term in the $1/N$ -expansion:

$$\begin{aligned} & \mathcal{S}_{\text{LO}}^{\text{eff.}}[\bar{\Psi}_\sigma, \Psi_\sigma] + \mathcal{S}_{\text{NLO}}^{\text{eff.}}[\bar{\Psi}_\sigma, \Psi_\sigma] \\ &= - \sum_{\sigma=\uparrow,\downarrow} \int dp \bar{\Psi}_\sigma(p) \left(i\omega - \frac{\mathbf{p}^2}{2m_{\text{F}}} + \mu_{\text{F}} \right) \Psi_\sigma(p) \\ & \quad + \frac{1}{2} \sum_{\sigma,\rho=\uparrow,\downarrow} \int \left(\prod_{i=1}^4 dp_i \right) \delta(p_4 + p_2 - p_1 - p_3) g_{\text{FF}} \bar{\Psi}_\sigma(p_1) \bar{\Psi}_\rho(p_3) \Psi_\rho(p_4) \Psi_\sigma(p_2), \end{aligned} \quad (60)$$

with the physical parameters of CF fields,

$$m_{\text{F}} = m_f + m_b, \quad (61)$$

$$\mu_{\text{F}} \simeq \epsilon_F = \frac{(3\pi^2 n_{\text{tot}})^{2/3}}{2m_{\text{F}}}, \quad (62)$$

$$g_{\text{FF}} \simeq -\frac{1}{N} \frac{2\pi a_{bf}}{m_{\text{R}}}. \quad (63)$$

Equation (60) is nothing but an action of two-component Fermi gases with weakly attractive four-Fermi interactions, which yields the BCS-paired state of fermions at low temperature. Thus we can expect that our system described by Eq.(60) also favor the BCS superfluidity of CFs (CF-BCS) below a transition temperature [27, 28],

$$T_{\text{C}}(\text{CF-BCS}) = \frac{\gamma}{\pi} \left(\frac{2}{e} \right)^{7/3} \epsilon_F \exp\left(\frac{\pi}{2k_{\text{F}} a_{\text{FF}}} \right), \quad (64)$$

with the Fermi momentum $k_{\text{F}} = \sqrt{2m_{\text{F}}\epsilon_F} = (3\pi^2 n_{\text{tot}})^{1/3}$ and the s-wave scattering length given by

$$\begin{aligned} a_{\text{FF}} &= \frac{m_{\text{F}}}{4\pi} g_{\text{FF}} \\ &= -\frac{1}{N} \frac{m_{\text{F}}}{2m_{\text{R}}} a_{bf}. \end{aligned} \quad (65)$$

Setting $N = 1$ yields the same result as derived in our previous work [7]. Note that the coefficient of a_{bf} in Eq.(65) becomes -2 for $N = 1$ with $m_b = m_f$, which is the same in magnitude but opposite in

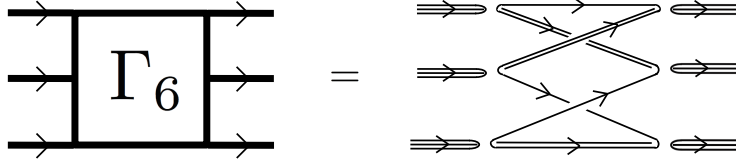


Figure 8: Graphical representation of the proper 6-point vertex of “bare” CF fields F_σ . In order to obtain the proper 6-point vertex of \mathcal{F}_σ , we need to multiply both sides by $(\sqrt{N})^6$, which comes from the normalization of six external legs ($\mathcal{F}_\sigma = \sqrt{N}F_\sigma$).

sign from the scattering length between bosonic dimers composed of spin-singlet fermion pairs within the same approximation. This is because our CFs are different in the statistics of their constituent particles from the composite bosons, so-called Cooper pairs, in two-component Fermi gases [5, 23, 24].

4.4 Higher order terms in the $1/N$ -expansion

We now consider the higher order terms in the $1/N$ -expansion of the CF action Eq.(20), especially focusing on the corrections to the effective four-Fermi.

Figure 8 shows a graphical representation of the proper 6-point vertex, based on the sextet term of CF fields in Eq.(20). We can see that the right hand side of Fig. 8 gives large N power-counting factors (i) N from an internal loop, (ii) $(1/N)^6$ from six vertices, and (iii) $(\sqrt{N})^6$ from the normalization ($\mathcal{F}_\sigma = \sqrt{N}F_\sigma$), which yield an $O(1/N^2)$ term as it should be in Eq.(20).

In general, we denote an $O(1/N^{n-1})$ term in Eq.(20) by $\mathcal{S}^{(n-1)}$ ($n \geq 2$), which is composed of $2n$ CF fields and the proper $2n$ -point vertex,

$$\begin{aligned} \mathcal{S}^{(n-1)}[\bar{\mathcal{F}}_\sigma, \mathcal{F}_\sigma] &= -\left(\frac{1}{N}\right)^{n-1} \frac{1}{n} \text{tr} \left[\int dw \sum_{\sigma=\uparrow, \downarrow} D(x, w) \mathcal{A}_\sigma(w, y) \right]^n \\ &= \frac{1}{n} \sum_{\sigma_1, \dots, \sigma_n=\uparrow, \downarrow} \int \left(\prod_{j=1}^n dp_{2j-1} dp_{2j} \right) \delta \left(\sum_{j=1}^n p_{2j} - \sum_{j=1}^n p_{2j-1} \right) \\ &\quad \times \Gamma_{2n}(\{p_i\}_{i=1}^{2n}) \left\{ \prod_{j=1}^n \bar{\mathcal{F}}_{\sigma_j}(p_{2j-1}) \mathcal{F}_{\sigma_j}(p_{2j}) \right\}. \end{aligned} \quad (66)$$

Here $\Gamma_{2n}(\{p_i\}_{i=1}^{2n})$ represents a proper $2n$ -point vertex of CF fields, defined by

$$\Gamma_{2n}(\{p_i\}_{i=1}^{2n}) = -\frac{1}{N^{n-1}} \int dq \prod_{j=1}^n D \left(\sum_{k=1}^{j-1} p_{2k-1} - \sum_{k=1}^{j-1} p_{2k} + q \right) S \left(\sum_{k=1}^j p_{2k} - \sum_{k=1}^{j-1} p_{2k-1} - q \right), \quad (67)$$

with a set of momenta $\{p_i\}_{i=1}^{2n} = \{p_1, p_2, \dots, p_{2n}\}$ constrained by the energy-momentum conservation, $\sum_{j=1}^n p_{2j} - \sum_{j=1}^n p_{2j-1} = 0$. Appendix A gives a detail derivation of the above expressions. Figure 9 shows a graphical representation of the proper $2n$ -point vertex. We can see that the right hand side of Fig. 9 gives large N power-counting factors (i) N from an internal loop, (ii) $(1/N)^{2n}$ from $2n$

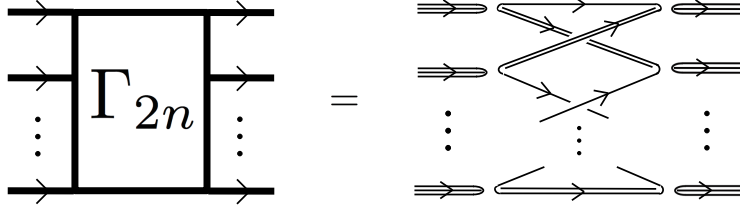


Figure 9: Graphical representation of the proper $2n$ -points vertex of “bare” CFs F_σ . In order to obtain the proper $2n$ -points vertex of \mathcal{F}_σ , we need to multiply both sides by $(\sqrt{N})^{2n}$, which comes from the normalization of $2n$ external legs ($\mathcal{F}_\sigma = \sqrt{N}F_\sigma$).

vertices, and (iii) $(\sqrt{N})^{2n}$ from the normalization ($\mathcal{F}_\sigma = \sqrt{N}F_\sigma$), which yield an $O(1/N^{n-1})$ term as is Γ_{2n} in Eq.(67). Comparing Eqs.(66), (67) with Eqs.(47), (48), we can easily check the consistency for the case of $n = 2$, *i.e.*, $\mathcal{S}^{(1)}[\bar{\mathcal{F}}_\sigma, \mathcal{F}_\sigma] = \mathcal{S}_{\text{NLO}}[\bar{\mathcal{F}}_\sigma, \mathcal{F}_\sigma]$.

Now let us consider diagrams higher order in the $1/N$ -expansion which contribute to the effective four-Fermi interaction. The leading-order contribution to the effective four-Fermi interaction is given by the proper 4-point vertex Γ_4 . Since our $1/N$ -expansion is equivalent to the loop expansion in terms of CF fields, the corrections to the proper 4-point vertex Γ_4 should start from one-loop graphs, as shown in Fig. 10 and 11. Figure 10 represents the contraction of the proper 6-point vertex Γ_6 , and its right hand side gives large N power-counting factors (i) N from an internal loop, (ii) $(1/N)^6$ from six vertices, and (iii) $(\sqrt{N})^6$ from the normalization ($\mathcal{F}_\sigma = \sqrt{N}F_\sigma$), which give an $O(1/N^2)$ term in total, *i.e.*, the next-to-leading-order contribution to the effective four-Fermi interaction. Figure 11 shows the shortest ladder diagram of the proper 4-point vertices Γ_4 , and its right hand side gives large N power-counting factors (i) N^2 from two internal loops, (ii) $(1/N)^8$ from eight vertices, and (iii) $(\sqrt{N})^8$ from the normalization ($\mathcal{F}_\sigma = \sqrt{N}F_\sigma$), which again yield an $O(1/N^2)$ term.

It is also possible to consider general $O(1/N^n)$ corrections based on the loop expansion in terms of CF fields which contribute to the effective four-Fermi interaction. Instead, we just remark that all the graphs are in the same order in terms of $n^{1/3}a_{bf}$, thus for $N = 1$ we need to sum up them to obtain the effective vertex function, as performed numerically in Refs [29–31].

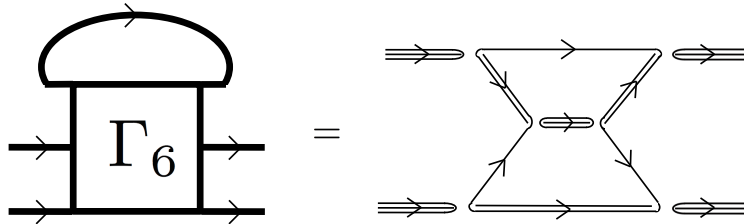


Figure 10: Graphical representation of the contraction of the proper 6-point vertex of “bare” CF fields F_σ , which contributes to the effective four-Fermi interaction.

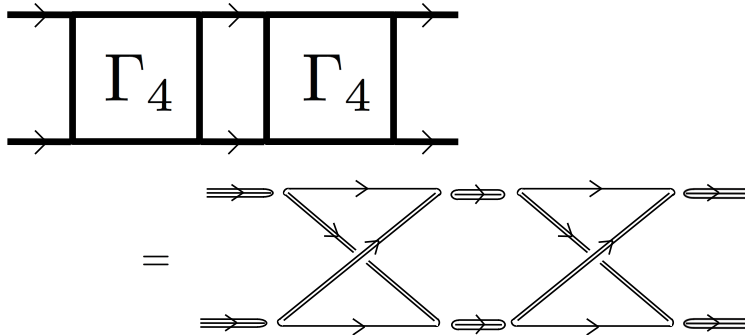


Figure 11: Graphical representation of the shortest ladder diagram of the proper 4-point vertices of “bare” CF fields F_σ , which contributes to the effective four-Fermi interaction.

5 Summary and discussion

We have investigated the large N expansion for strongly-coupled boson-fermion mixtures, proposed in Ref. [7]. We first derived a theory equivalent to the original boson-fermion mixture, which is described by composite fermions (CFs). The $1/N$ -expansion naturally appears in the quantum theory of CFs. We showed that the leading-order terms in the $1/N$ -expansion yield a low energy effective action of CFs which is equivalent to that of a two-component free Fermi gas. The next-to-leading-order term was also estimated, and it turned out that the effective action up to the NLO reduces to an action of a weakly-interacting two-component Fermi gas. Thus we concluded that there is the BCS superfluidity of CFs below $T_C(\text{CF-BCS})$ given by Eq.(64) in our large N model. Also we discussed how to estimate the higher order terms in the $1/N$ -expansion, where the diagrammatic representation provides simple explanations for power-counting of the $1/N$ factors.

Finally, we would like to mention important similarities between our boson-fermion mixtures and hadron physics. Table 1 summarizes the correspondence in components between ultracold atoms and dense QCD, both of which can be considered as boson-fermion mixtures with $N = 1$ in our model [6–8]. Note that it is known that the effective interaction between nucleons is not so strong as the original gluonic interaction between quarks. For example, the energy gap in nuclear matter, *i.e.*, superfluid matter of nucleons, is at most a few MeV [32], while the energy gap in color-superconductivity is from 10 to 10^2 times larger [33]. This is consistent with our results which show that the weakly-coupled CF system can be derived from the strongly-coupled boson-fermion mixture. However, our model seems too simple to relate its results to various phenomena in QCD. Furthermore, chiral symmetry breaking plays an important role in hadron physics [6], which does not appear in nonrelativistic systems. Keeping these observations in mind, we suggest that both theoretical and experimental

Table 1: Correspondence between the boson-fermion mixture in ultracold atoms and the diquark-quark mixture in dense QCD.

Our Notations	Ultra-Cold Atoms	Dense QCD
ϕ	bosonic atom (e.g., ^{87}Rb)	diquark
$\psi_\uparrow, \psi_\downarrow$	fermionic atoms (e.g., ^{40}K)	unpaired quarks
$\Psi_\uparrow, \Psi_\downarrow$	composite fermions (boson-fermion dimers)	nucleons (baryons)
g_{bf}	boson-fermion attraction	gluonic attraction
$\langle \Psi_\uparrow \Psi_\downarrow \rangle \neq 0$	composite-fermion superfluidity	nucleon superfluidity

studies in boson-fermion mixtures provide a new tool to investigate properties of dense QCD, which is not readily observable in laboratory experiments.

Acknowledgements

The author thanks G. Baym, D. Blaschke, T. Hatsuda, S. Uchino for fruitful discussions. This research was supported by JSPS Research Fellowship for young scientists.

A Fourier transformations

The definitions of Fourier transforms used in our main text are given by

$$\mathcal{F}_\sigma(x) = \int dp e^{ipx} \mathcal{F}_\sigma(p), \quad (68)$$

$$\bar{\mathcal{F}}_\sigma(x) = \int dp e^{-ipx} \bar{\mathcal{F}}_\sigma(p), \quad (69)$$

$$D(x, y) = \int dq e^{iq(x-y)} D(q), \quad (70)$$

$$S(x, y) = \int dq e^{iq(x-y)} S(q), \quad (71)$$

with an inner product: $ipx = i\omega\tau - i\mathbf{p} \cdot \mathbf{x}$ where ω and \mathbf{p} denote the Matsubara frequency and spatial momentum vector, respectively. For simplicity, we have used notations: $p = (\mathbf{p}, i\omega)$, $\int dp = T \sum_\omega \int d\mathbf{p} / (2\pi)^3$. We adopt a convention which distinguishes functions from their Fourier transforms only by their arguments. Correspondingly, the Fourier transform of the quadratic term in Eq.(22) becomes

$$\begin{aligned} & \int dx dw \bar{\mathcal{F}}_\sigma(x) D(x, w) S(x, w) \mathcal{F}_\sigma(w) \\ &= \int dp_1 dp_2 dq_1 dq_2 \delta(q_1 + q_2 - p_1) \delta(p_2 - q_1 - q_2) \bar{\mathcal{F}}_\sigma(p_1) D(q_1) S(q_2) \mathcal{F}_\sigma(p_2) \\ &= \int dp \bar{\mathcal{F}}_\sigma(p) \left[\int dq D(q) S(p - q) \right] \mathcal{F}_\sigma(p). \end{aligned} \quad (72)$$

Also, the quartic term in Eq.(47) transforms as

$$\begin{aligned}
& -\frac{1}{N} \int dx dv dw dz D(x, w) \bar{\mathcal{F}}_\sigma(v) S(v, w) \mathcal{F}_\sigma(w) D(v, z) \bar{\mathcal{F}}_\rho(x) S(x, z) \mathcal{F}_\rho(z) \\
& = -\frac{1}{N} \int \left(\prod_{i=1}^4 dp_i dq_i \right) \delta(q_1 + q_4 - p_3) \delta(p_2 - q_1 - q_2) \delta(q_2 + q_3 - p_1) \delta(p_4 - q_3 - q_4) \\
& \quad \times D(q_1) \bar{\mathcal{F}}_\sigma(p_1) S(q_2) \mathcal{F}_\sigma(p_2) D(q_3) \bar{\mathcal{F}}_\rho(p_3) S(q_4) \mathcal{F}_\rho(p_4) \\
& = \int \left(\prod_{i=1}^4 dp_i \right) \delta(p_4 + p_2 - p_1 - p_3) \Gamma(\{p_i\}_{i=1}^4) \bar{\mathcal{F}}_\sigma(p_1) \bar{\mathcal{F}}_\rho(p_3) \mathcal{F}_\rho(p_4) \mathcal{F}_\sigma(p_2), \tag{73}
\end{aligned}$$

where $\Gamma(\{p_i\}_{i=1}^4)$ represents a proper 4-point vertex of composite fermions, defined by

$$\Gamma(\{p_i\}_{i=1}^4) = -\frac{1}{N} \int dq D(q) S(p_2 - q) D(p_1 - p_2 + q) S(p_3 - q), \tag{74}$$

with a set of momenta $\{p_i\}_{i=1}^4 = \{p_1, p_2, p_3, p_4\}$.

We can write down a general $2n$ -point vertex function explicitly in its Fourier transform,

$$\begin{aligned}
& -\frac{1}{N^{n-1}} \text{tr} \left[\int dw \sum_{\sigma=\uparrow, \downarrow} D(x, w) \mathcal{A}_\sigma(w, y) \right]^n \tag{75} \\
& = -\frac{1}{N^{n-1}} \sum_{\sigma_1, \dots, \sigma_n = \uparrow, \downarrow} \int \left(\prod_{i=1}^{2n+1} dx_i \right) \delta(x_1 - x_{2n+1}) \left\{ \prod_{j=1}^n D(x_{2j-1}, x_{2j}) \bar{\mathcal{F}}_{\sigma_j}(x_{2j+1}) S(x_{2j+1}, x_{2j}) \mathcal{F}_{\sigma_j}(x_{2j}) \right\} \\
& = -\frac{1}{N^{n-1}} \sum_{\sigma_1, \dots, \sigma_n = \uparrow, \downarrow} \int \left(\prod_{j=1}^n dq_{2j-1} dq_{2j} dp_{2j-1} dp_{2j} \right) \\
& \quad \delta(q_1 + q_{2n} - p_{2n-1}) \left\{ \prod_{j=1}^n \delta(p_{2j} - q_{2j} - q_{2j-1}) \right\} \left\{ \prod_{j=1}^{n-1} \delta(q_{2j+1} + q_{2j} - p_{2j-1}) \right\} \\
& \quad \times \left\{ \prod_{j=1}^n D(q_{2j-1}) S(q_{2j}) \right\} \left\{ \prod_{j=1}^n \bar{\mathcal{F}}_{\sigma_j}(p_{2j-1}) \mathcal{F}_{\sigma_j}(p_{2j}) \right\} \\
& = -\frac{1}{N^{n-1}} \sum_{\sigma_1, \dots, \sigma_n = \uparrow, \downarrow} \int \left(\prod_{j=1}^n dp_{2j-1} dp_{2j} \right) \delta \left(\sum_{j=1}^n p_{2j} - \sum_{j=1}^n p_{2j-1} \right) \\
& \quad \times \left\{ \int dq_1 \prod_{j=1}^n D \left(\sum_{k=1}^{j-1} p_{2k-1} - \sum_{k=1}^{j-1} p_{2k} + q_1 \right) S \left(\sum_{k=1}^j p_{2k} - \sum_{k=1}^{j-1} p_{2k-1} - q_1 \right) \right\} \left\{ \prod_{j=1}^n \bar{\mathcal{F}}_{\sigma_j}(p_{2j-1}) \mathcal{F}_{\sigma_j}(p_{2j}) \right\} \\
& = \sum_{\sigma_1, \dots, \sigma_n = \uparrow, \downarrow} \int \left(\prod_{j=1}^n dp_{2j-1} dp_{2j} \right) \delta \left(\sum_{j=1}^n p_{2j} - \sum_{j=1}^n p_{2j-1} \right) \Gamma_{2n}(\{p_i\}_{i=1}^{2n}) \left\{ \prod_{j=1}^n \bar{\mathcal{F}}_{\sigma_j}(p_{2j-1}) \mathcal{F}_{\sigma_j}(p_{2j}) \right\},
\end{aligned}$$

where $\Gamma_{2n}(\{p_i\}_{i=1}^{2n})$ represents the proper $2n$ -point vertex of composite fermions, defined by

$$\Gamma_{2n}(\{p_i\}_{i=1}^{2n}) = -\frac{1}{N^{n-1}} \int dq \prod_{j=1}^n D \left(\sum_{k=1}^{j-1} p_{2k-1} - \sum_{k=1}^{j-1} p_{2k} + q \right) S \left(\sum_{k=1}^j p_{2k} - \sum_{k=1}^{j-1} p_{2k-1} - q \right), \tag{76}$$

with a set of momenta $\{p_i\}_{i=1}^{2n} = \{p_1, p_2, \dots, p_{2n}\}$.

B Derivative expansion of the inverse propagator for composite fermions at $T = 0$

We will give details on the derivation of Eq.(30) and Eqs.(32)-(34) in the derivative expansion of $G^{-1}(p)$ at zero temperature. We can formally perform a real-time analysis by replacing our Matsubara frequency $i\omega$ with a continuous energy variable E at zero temperature. Using a four-momentum in real-time formalism; (\mathbf{p}, E) , we have a real-time form of Eq.(29) at zero temperature,

$$\begin{aligned} G^{-1}(\mathbf{p}, E) &= \frac{m_R}{2\pi a_{bf}} - \int \frac{d\mathbf{q}}{(2\pi)^3} \left\{ \frac{1}{\varepsilon(\mathbf{q})} - \frac{1}{\xi_f(\mathbf{p} - \mathbf{q}) + \xi_b(\mathbf{q}) - E} \right\} \\ &= \frac{m_R}{2\pi a_{bf}} - \int \frac{d\mathbf{q}}{(2\pi)^3} \left\{ \frac{1}{\varepsilon(\mathbf{q})} - \frac{1}{\varepsilon(\mathbf{q}) - \mathbf{p} \cdot \mathbf{q}/m_f + p^2/(2m_f) - E - (\mu_b + \mu_f)} \right\} \\ &= \frac{m_R}{2\pi a_{bf}} - I_1. \end{aligned} \quad (77)$$

Here we used the fact that $n_b(\mathbf{q})$ and $n_f(\mathbf{p} - \mathbf{q})$ vanishes at $T = 0$ under our assumption: $\mu_b < 0$ and $\mu_f < 0$, and we denoted an integral in Eq.(77) by I_1 , which becomes

$$\begin{aligned} I_1 &= \int \frac{d\mathbf{q}}{(2\pi)^3} \left\{ \frac{1}{\varepsilon(\mathbf{q})} - \frac{1}{\varepsilon(\mathbf{q}) - \mathbf{p} \cdot \mathbf{q}/m_f + p^2/(2m_f) - E + |\mu|} \right\} \\ &= \frac{1}{4\pi^2} \int_0^\Lambda q^2 dq \int_{-1}^1 d\cos\theta \left\{ \frac{1}{\varepsilon(\mathbf{q})} - \frac{1}{\varepsilon(\mathbf{q}) - pq \cos\theta/m_f + A} \right\} \\ &= \frac{m_R \Lambda}{\pi^2} - \frac{1}{4\pi^2} \int_0^\Lambda q^2 dq \frac{m_f}{pq} \ln \left| \frac{pq/m_f + \varepsilon(\mathbf{q}) + A}{-pq/m_f + \varepsilon(\mathbf{q}) + A} \right|, \end{aligned} \quad (78)$$

with $p = |\mathbf{p}|$, $q = |\mathbf{q}|$, $\mu = \mu_b + \mu_f (< 0)$, and $A = p^2/(2m_f) - E + |\mu|$. As we will see below, I_1 yields a finite value even in the limit of $\Lambda \rightarrow \infty$. We can rewrite terms in the logarithm in Eq.(78) as

$$\begin{aligned} \frac{pq}{m_f} + \varepsilon(\mathbf{q}) + A &= \frac{1}{2m_R} \left(q^2 + 2\frac{m_R}{m_f} pq \right) + \frac{p^2}{2m_f} - E + |\mu| \\ &= \frac{1}{2m_R} \{ (q + \alpha p)^2 + 2m_R A' \}, \end{aligned} \quad (79)$$

and

$$-\frac{pq}{m_f} + \varepsilon(\mathbf{q}) + A = \frac{1}{2m_R} \{ (q - \alpha p)^2 + 2m_R A' \}, \quad (80)$$

with a mass-ratio parameter $\alpha = m_R/m_f$, and $A' = p^2/[2(m_b + m_f)] - E + |\mu|$. Then, Eq.(78) reads

$$I_1 = \frac{m_R \Lambda}{\pi^2} - \frac{m_f}{4\pi^2 p} \int_0^\Lambda dq q \ln \left| \frac{(q + \alpha p)^2 + 2m_R A'}{(q - \alpha p)^2 + 2m_R A'} \right|. \quad (81)$$

By employing the following integral formula:

$$\begin{aligned} &\int dx x \ln \left| \frac{(x+a)^2 + b}{(x-a)^2 + b} \right| \\ &= \left(\frac{x^2 - a^2 + b}{2} \right) \ln \left| \frac{(x+a)^2 + b}{(x-a)^2 + b} \right| + 2ax - 2a\sqrt{|b|} \left\{ \tan^{-1} \left(\frac{x+a}{\sqrt{|b|}} \right) + \tan^{-1} \left(\frac{x-a}{\sqrt{|b|}} \right) \right\}, \end{aligned} \quad (82)$$

we can perform the integration in Eq.(78),

$$\begin{aligned}
I_1 &= \frac{m_R \Lambda}{\pi^2} - \frac{m_f}{4\pi^2 p} \left\{ \frac{\Lambda^2 - (\alpha p)^2 + 2m_R A'}{2} \right\} \ln \left| \frac{(\Lambda + \alpha p)^2 + 2m_R A'}{(\Lambda - \alpha p)^2 + 2m_R A'} \right| \\
&\quad - \frac{m_f}{4\pi^2 p} 2\alpha p \Lambda + \frac{m_f}{4\pi^2 p} 2\alpha p \sqrt{|2m_R A'|} \left\{ \tan^{-1} \left(\frac{\Lambda + \alpha p}{\sqrt{|2m_R A'|}} \right) + \tan^{-1} \left(\frac{\Lambda - \alpha p}{\sqrt{|2m_R A'|}} \right) \right\} \\
&= \frac{m_R \Lambda}{\pi^2} - \frac{m_f}{4\pi^2 p} \left(\frac{\Lambda^2 - \alpha^2 p^2 + 2m_R A'}{2} \right) \ln \left| \frac{(\Lambda + \alpha p)^2 + 2m_R A'}{(\Lambda - \alpha p)^2 + 2m_R A'} \right| \\
&\quad - \frac{m_R \Lambda}{2\pi^2} + \frac{m_R}{2\pi^2} \sqrt{|2m_R A'|} \left\{ \tan^{-1} \left(\frac{\Lambda + \alpha p}{\sqrt{|2m_R A'|}} \right) + \tan^{-1} \left(\frac{\Lambda - \alpha p}{\sqrt{|2m_R A'|}} \right) \right\}. \tag{83}
\end{aligned}$$

Noting that the cutoff Λ is the largest scale in our model and also that we are interested in the low-energy and low-momentum regime, let us expand the logarithm and arctangent functions in Eq.(83).

As for the logarithm function, the power-series formula, $\ln(1+x) = \sum_{n=1}^{\infty} (-1)^{n-1} x^n/n$, gives

$$\begin{aligned}
&\left(\frac{\Lambda^2 - \alpha^2 p^2 + 2m_R A'}{2} \right) \ln \left| \frac{(\Lambda + \alpha p)^2 + 2m_R A'}{(\Lambda - \alpha p)^2 + 2m_R A'} \right| \\
&= \frac{\Lambda^2}{2} \left(1 - \frac{\alpha^2 p^2 - 2m_R A'}{\Lambda^2} \right) \ln \left| \frac{1 + 2\alpha p/\Lambda + (\alpha^2 p^2 + 2m_R A')/\Lambda^2}{1 - 2\alpha p/\Lambda + (\alpha^2 p^2 + 2m_R A')/\Lambda^2} \right| \\
&= \frac{\Lambda}{2} \left(1 - \frac{\alpha^2 p^2 - 2m_R A'}{\Lambda^2} \right) \left\{ 4\alpha p + O \left(\frac{\alpha p (\alpha^2 p^2 + 2m_R A')}{\Lambda^2} \right) \right\} \\
&= 2\alpha p \Lambda + O \left(\frac{\alpha p (\alpha^2 p^2 \pm 2m_R A')}{\Lambda} \right), \tag{84}
\end{aligned}$$

while the formula for the arctangent function: $\tan^{-1}(x) = \pi/2 - \tan^{-1}(1/x)$, yields

$$\tan^{-1} \left(\frac{\Lambda + \alpha p}{\sqrt{|2m_R A'|}} \right) + \tan^{-1} \left(\frac{\Lambda - \alpha p}{\sqrt{|2m_R A'|}} \right) = \pi + O \left(\frac{\sqrt{|2m_R A'|}}{\Lambda \pm \alpha p} \right), \tag{85}$$

which finally give an explicit form of I_1 within the derivative expansion,

$$\begin{aligned}
I_1 &= \frac{m_R \Lambda}{\pi^2} - \frac{m_R \Lambda}{2\pi^2} - \frac{m_R \Lambda}{2\pi^2} + \frac{m_R}{2\pi} \sqrt{|2m_R A'|} + O \left(\frac{\alpha p (\alpha^2 p^2 \pm 2m_R A')}{\Lambda} \right) + O \left(\frac{\sqrt{|2m_R A'|}}{\Lambda \pm \alpha p} \right) \\
&= \frac{(2m_R)^{3/2}}{4\pi} \sqrt{|A'|} + O \left(\frac{\alpha p (\alpha^2 p^2 \pm 2m_R A')}{\Lambda} \right) + O \left(\frac{\sqrt{|2m_R A'|}}{\Lambda \pm \alpha p} \right). \tag{86}
\end{aligned}$$

Substituting Eq.(86) into Eq.(77) yields

$$G^{-1}(\mathbf{p}, E) \simeq \frac{m_R}{2\pi a_{bf}} - \frac{(2m_R)^{3/2}}{4\pi} \sqrt{|\mu| + \frac{\mathbf{p}^2}{2(m_b + m_f)} - E}, \tag{87}$$

which finally gives the derivative expansion of G^{-1} in terms of $\{\mathbf{p}^2/[2(m_b + m_f)] - E\}/|\mu|$ under the assumption sated in the main text,

$$\begin{aligned}
G^{-1}(\mathbf{p}, E) &\simeq \frac{m_R}{2\pi a_{bf}} - \frac{(2m_R)^{3/2}}{4\pi} \sqrt{|\mu|} \left(1 + \frac{\mathbf{p}^2/[2(m_b + m_f)] - E}{|\mu|} \right)^{1/2} \\
&\simeq \frac{m_R}{2\pi a_{bf}} (1 - a_{bf} \sqrt{2m_R} |\mu|) - \frac{1}{2\pi} \frac{m_R}{2(m_b + m_f)} \sqrt{\frac{m_R}{2|\mu|}} \mathbf{p}^2 + \frac{m_R}{2\pi} \sqrt{\frac{m_R}{2|\mu|}} E. \tag{88}
\end{aligned}$$

The above expression corresponds to Eq.(31) with the coefficients a, c, d given by Eq.(32)-(34).

References

- [1] J. Bardeen, G. Baym, and D. Pines, Phys. Rev. **156**, 207 (1967).
- [2] M. J. Bijlsma, B. A. Heringa, and H. T. C. Stoof, Phys. Rev. A **61**, 053601 (2000).
- [3] H. Heiselberg, C. J. Pethick, H. Smith, and L. Viverit, Phys. Rev. Lett. **85**, 2418 (2000).
- [4] A. Storozhenko, P. Schuck, T. Suzuki, H. Yabu, and J. Dukelsky, Phys. Rev. A **71**, 063617 (2005).
- [5] M. Yu. Kagan, I. V. Brodsky, D. V. Efremov, and A. V. Klapptsov, Phys. Rev. A **70**, 023607 (2004).
- [6] G. Baym, T. Hatsuda, M. Tachibana, and N. Yamamoto, J. Phys. G **35**, 104021 (2008).
- [7] K. Maeda, G. Baym, and T. Hatsuda, Phys. Rev. Lett. **103**, 085301 (2009).
- [8] T. Hatsuda and K. Maeda, arXiv:0912.1437[hep-ph].
Chapter of the book: *Understanding Quantum Phase transitions*, edited by L. D. Carr (CRC Press, Taylor and Francis, 2010).
- [9] H. Feshbach, Ann. Phys. (N.Y.) **5**, 357 (1958); **19**, 287 (1962).
- [10] T. Köhler, K. Góral, and P. S. Julienne, Rev. Mod. Phys. **78**, 1311 (2006).
- [11] I. Bloch, J. Dalibard, and W. Zwerger, Rev. Mod. Phys. **80**, 885 (2008).
- [12] C. Ospelkaus, S. Ospelkaus, L. Humbert, P. Ernst, K. Sengstock, and K. Bongs, Phys. Rev. Lett. **97**, 120402 (2006).
- [13] J. J. Zirbel, K. -K. Ni, S. Ospelkaus, J. P. D’Incao, C. E. Wieman, J. Ye, and D. S. Jin, Phys. Rev. Lett. **100**, 143201 (2008).
- [14] G. Baym, J.-P. Blaizot, and J. Zinn-Justin, Europhys. Lett. **49**, 150 (2000).
- [15] P. Arnold, G. Moore, and B. Tomášik, Phys. Rev. A **65**, 013606 (2001).
- [16] P. Nikolić and S. Sachdev, Phys. Rev. A **75**, 033608 (2007).
- [17] M. Y. Veillette, D. E. Sheehy, and L. Radzihovsky, Phys. Rev. A **75**, 043614 (2007).
- [18] H. Abuki and T. Brauner, Phys. Rev. A **78**, 125010 (2008).
- [19] M. Moshe and J. Zinn-Justin, Phys. Rept. **385**, 69 (2003).

- [20] C. J. Pethick and H. Smith, *Bose-Einstein Condensation in Dilute Gases* (Cambridge University Press, Cambridge, 2008).
- [21] L. J. Abu-Raddad, A. Hosaka, D. Ebert, and H. Toki, *Phys. Rev. D* **66**, 025206 (2002).
- [22] J. W. Negele and H. Orland, *Quantum Many-particle systems* (Westview Press, Boulder, 1988).
- [23] C. A. R. Sá de Melo, M. Randeria, and J. R. Engelbrecht, *Phys. Rev. Lett.* **71**, 3202 (1993).
- [24] R. Haussmann, *Z. Phys. B: Condens. Matter* **91**, 291 (1993).
- [25] F. Pistolesi and G. C. Strinati, *Phys. Rev. B* **53**, 15168 (1996).
- [26] P. Pieri and G. C. Strinati, *Phys. Rev. B* **61**, 15370 (2000).
- [27] J. Bardeen, L. N. Cooper, and J. R. Schrieffer, *Phys. Rev.* **106**, 162 (1957).
- [28] L. P. Gor'kov and T. K. Melik-Barkhudarov, *Sov. Phys. JETP* **13**, 1081 (1961).
- [29] D. S. Petrov, C. Salomon, and G. V. Shlyapnikov, *Phys. Rev. Lett.* **93**, 090404 (2004); *Phys. Rev.* **A71**, 012708 (2005); *J. Phys. B*, **38**, S645 (2005); arXiv:0810.1949 [cond-mat].
- [30] I. V. Brodsky, M. Yu. Kagan, A. V. Klaptsov, R. Combescot, and X. Leyronas, *Phys. Rev.* **A73**, 032724 (2006).
- [31] J. Levinsen and V. Gurarie, *Phys. Rev.* **A73**, 053607 (2006).
- [32] D. J. Dean and M. Hjorth-Jensen, *Rev. Mod. Phys.* **75**, 607 (2003).
- [33] M. G. Alford, A. Schmitt, K. Rajagopal, and T. Schafer, *Rev. Mod. Phys.* **80**, 1455 (2008).